

New Pupil Masks for High-Contrast Imaging

Robert J. Vanderbei^a, N. Jeremy Kasdin^a, David N. Spergel^a, and Marc Kuchner^d

^aPrinceton University, Princeton, NJ

^dHarvard-Smithsonian Ctr. For Astrophysics, Cambridge, MA

ABSTRACT

Motivated by the desire to image exosolar planets, recent work by us and others has shown that high-contrast imaging can be achieved using specially shaped pupil masks. To date, our masks have been symmetric with respect to a cartesian coordinate system but were not rotationally invariant, thus requiring that one take multiple images at different angles of rotation about the central point in order to obtain high-contrast in all directions. In this talk, we present two new classes of masks that have rotational symmetry and provide high-contrast in all directions with just one image. These masks provide the required 10^{-10} level of contrast to within $4\lambda/D$ of the central point. They are also well-suited for use on ground-based telescopes, and perhaps NGST as well, since they can accommodate central obstructions and associated support spiders.

1. APODIZATION

The purpose of this paper is to present and compare new pupil plane masks for high-contrast imaging in the context of designing the Terrestrial Planet Finder (TPF) space telescope. Since pupil plane masks can be viewed mathematically a special case of apodized pupils, we begin by developing some notation and concepts in the general context of pupil apodization.

The image-plane *electric field* $E(\rho)$ produced by an on-axis point source and an apodized aperture defined by a circularly-symmetric *apodization function* $A(r)$ is itself circularly symmetric and is given by

$$\begin{aligned} E(\rho) &= \int_0^{1/2} \int_0^{2\pi} e^{-2\pi i r \rho \cos(\theta-\phi)} A(r) r d\theta dr, \\ &= 2\pi \int_0^{1/2} J_0(2\pi r \rho) A(r) r dr, \end{aligned} \quad (1)$$

where J_0 denotes the 0-th order Bessel function of the first kind, r and θ denote polar coordinates in the pupil plane, and ρ and ϕ denote polar coordinates in the image plane. Angles θ and ϕ are measured in radians. The unitless pupil-plane “length” r is given as a multiple of the aperture D . The unitless image-plane “length” ρ is given as a multiple of focal-length times wavelength over aperture ($f\lambda/D$) or, equivalently, as an angular measure on the sky, in which case it is a multiple of just λ/D . The *point spread function* (psf) is the square of the electric field.

1.1. Performance Metrics

As we discuss the relative merits of various pupil designs, there are a few performance metrics to keep in mind. The first is *contrast*, which is a function of radial position in the image plane. It is given by

$$E^2(\rho)/E^2(0).$$

Paradoxically, we say that we have high-contrast when this ratio is very small. For TPF, the consensus is that a contrast of 10^{-10} is necessary in order to image an Earth-like planet that is 1 AU from its Sun-like star.

Further author information: (Send correspondence to R.J.V.)

R.J.V.: E-mail: rvdb@princeton.edu, Telephone: 1 609 258 0876, Dept.: Operations Research and Financial Engineering

N.J.K.: E-mail: jkasdin@princeton.edu, Telephone: 1 609 258 5673, Dept.: Mechanical and Aerospace Engineering

D.N.S.: E-mail: dns@princeton.edu, Telephone: 1 609 258 3589, Dept.: Astrophysical Sciences

M.K.: E-mail: mkuchner@cfa.harvard.edu, Telephone: 1 617 496 4773,

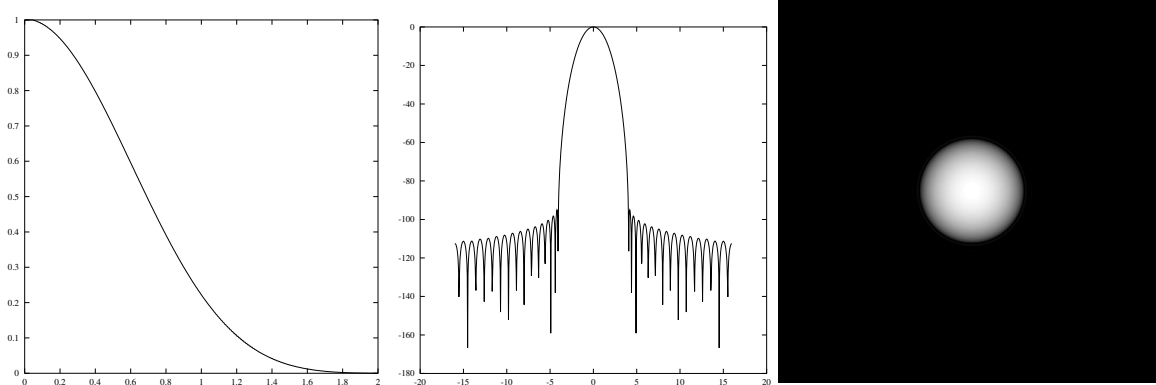


Figure 1. *Left.* The generalized prolate spheroidal apodization. *Center and Right.* The corresponding point-spread function. Note that high-contrast (10^{-10}) extends from $\rho_{iwa} = 4$ to infinity. The Airy throughput is 9%.

The second metric is the *inner working angle*, ρ_{iwa} and, of lesser importance, the *outer working angle*, ρ_{owa} . We wish to design pupil masks that have high-contrast for all ρ 's in the interval $\rho_{iwa} \leq \rho \leq \rho_{owa}$.

The third performance metric is *Airy throughput*. It is defined as the energy that falls into the main lobe of the psf measured relative to the total energy conveyed through a fully open aperture:

$$\frac{\int_0^{\rho_{iwa}} E^2(\rho) 2\pi \rho d\rho}{(\pi(1/2)^2)} = 8 \int_0^{\rho_{iwa}} E^2(\rho) \rho d\rho.$$

1.2. Generalized Prolate Spheroidal Wave Function

One of the important apodization functions is Slepian's *generalized prolate spheroidal wave function*.¹ It is defined as the solution to the following optimization problem:

$$\text{maximize } \frac{\int_0^{\rho_{iwa}} E(\rho)^2 \rho d\rho}{\int_0^{\infty} E(\rho)^2 \rho d\rho}.$$

An equivalent but computationally easier formulation is this:

$$\begin{aligned} &\text{minimize } \int_{\rho_{iwa}}^{\infty} E(\rho)^2 \rho d\rho \\ &\text{subject to } A(0) = 1. \end{aligned}$$

Choosing $\rho_{iwa} = 4$ provides 10^{-10} contrast for $\rho \geq \rho_{iwa}$. Its Airy throughput is 9%. Fig. 1 shows the apodization and its associated psf.

1.3. Finite Outer Working Angle

It is computationally easier and physically more compelling to design a pupil that provides high contrast between some *inner working angle* and a finite *outer working angle*. An optimization problem that accomplishes this is:

$$\begin{aligned} &\text{maximize } \int_0^{1/2} A(r) 2\pi r dr \\ &\text{subject to } -10^{-5} E(0) \leq E(\rho) \leq 10^{-5} E(0), \quad \rho_{iwa} \leq \rho \leq \rho_{owa}, \\ & \quad \quad \quad 0 \leq A(r) \leq 1, \quad \quad \quad 0 \leq r \leq 1/2, \end{aligned}$$

Interestingly, the solution turns out to be zero-one valued. That is, it is a *pupil mask* consisting of concentric rings. The number of rings tends to infinity as $\rho_{owa} \rightarrow \infty$,

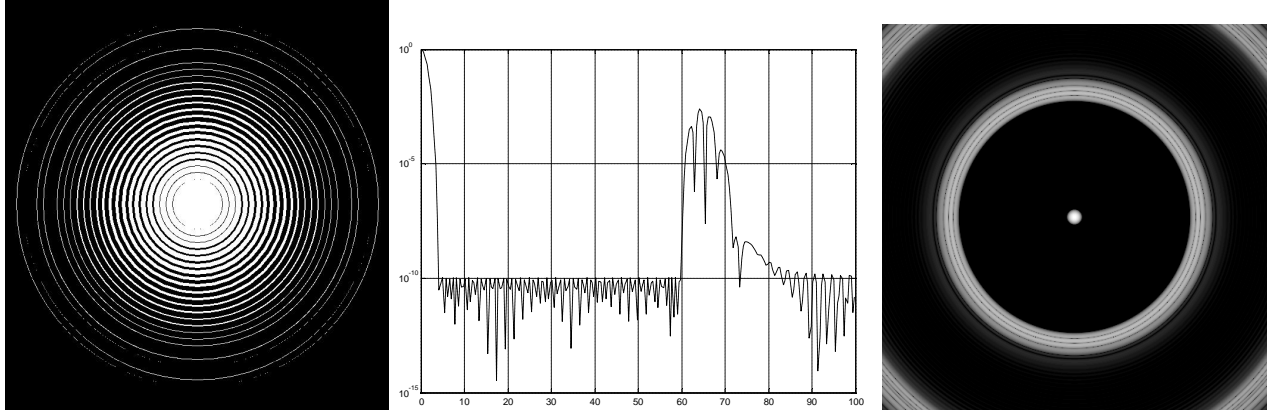


Figure 2. *Left.* A concentric ring mask designed for $\rho_{iwa} = 4$ and $\rho_{owa} = 60$. *Center and Right.* The associated psf. Note: the Airy throughput is 9%.

2. PUPIL MASKS

2.1. Concentric Ring Masks

At the end of the previous section, we saw that concentric ring masks are the optimal solution to a particular optimization problem. Fig. 2 shows the optimal concentric ring mask for $\rho_{iwa} = 4$ and $\rho_{owa} = 60$. Note that there is a bright set of diffraction rings extending from $\rho = 60$ to about $\rho = 80$. It turns out this design, and in fact designs in general that have a finite outer working angle, put about half of the transmitted light into the Airy disk and the other half into the outer regions. The Airy throughput for this mask is 9% (and the total throughput, which equals the open area, is about 18%).

2.2. Spiderweb Masks

In order to build a concentric ring mask, one needs a means of supporting the rings. It is felt that glass cannot be used because of the inevitable scatter that would result. The only alternative is to use a spider vane structure. Consider N “pie-shaped” spider vanes each of width α :

$$S_n = \left\{ (r, \theta) : 0 \leq r \leq 1/2, \frac{2\pi n}{N} + \frac{\alpha}{2} \leq \theta \leq \frac{2\pi(n+1)}{N} - \frac{\alpha}{2} \right\}, \quad n = 0, 1, \dots, N-1.$$

As shown in Ref. 2, overlaying these spider vanes on an apodization $A(r)$ yields the following electric field:

$$\begin{aligned} E(\rho, \phi) = & (2\pi - N\alpha) \int_0^{1/2} J_0(2\pi r \rho) A(r) r dr \\ & - 4 \sum_{j=1}^{\infty} \int_0^{1/2} J_{jN}(2\pi r \rho) \cos(jN(\phi - \pi/2)) \frac{1}{j} \sin(jN \frac{\alpha}{2}) A(r) r dr. \end{aligned}$$

It is also shown in Ref. 2 that, for N large and ρ not very large, the first term in the infinite sum dominates the rest. Hence, the electric field can be approximated by a combination of just two Bessel integrals:

$$\begin{aligned} E(\rho, \phi) \approx & 2\pi \int_0^{1/2} J_0(2\pi r \rho) (1 - N\alpha/(2\pi)) A(r) r dr \\ & - 4 \int_0^{1/2} J_N(2\pi r \rho) \cos(N(\phi - \pi/2)) \sin(N \frac{\alpha}{2}) A(r) r dr. \end{aligned} \quad (2)$$

Note that the first term is just the original electric field given in Eq. 1 reduced by a factor of $1 - N\alpha/(2\pi)$, which is just the fraction of the aperture that remains uncovered by the spiders. The second term produces the well-known diffraction

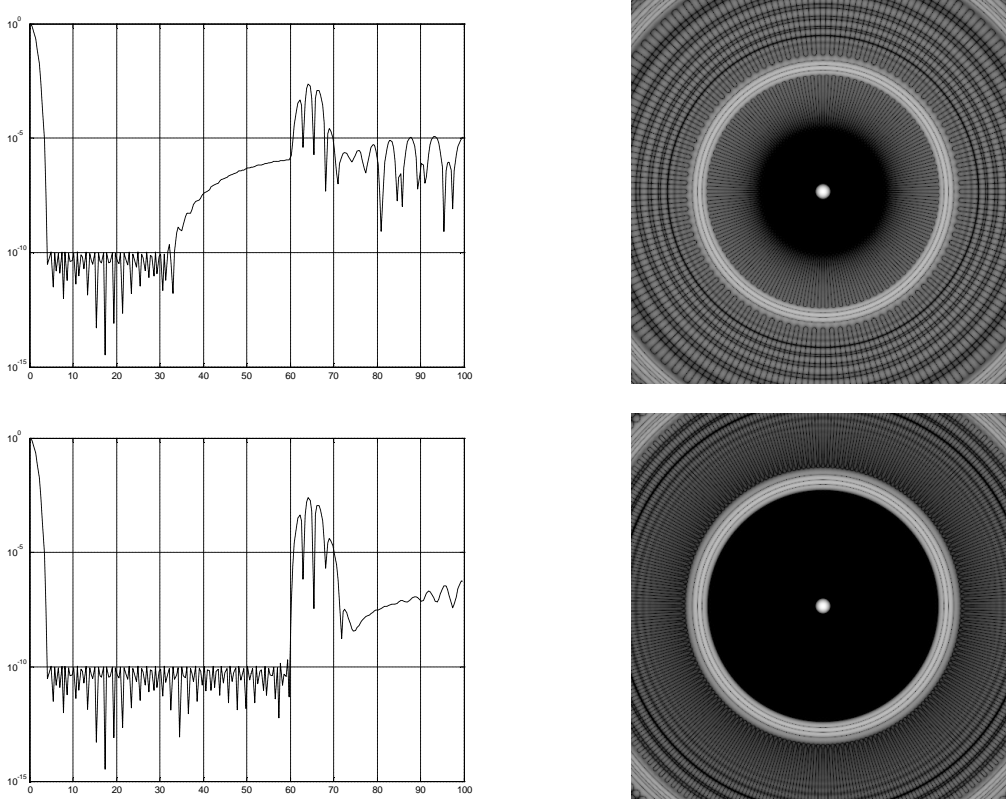


Figure 3. *Top.* The psf for a spiderweb mask with $rhonaught = 4$, $\rho_{owa} = 60$, and $N = 100$ vanes. *Bottom.* The psf for a spiderweb mask with $rhonaught = 4$, $\rho_{owa} = 60$, and $N = 180$ vanes.

spikes. As we know, using a small number of spider vanes makes bright diffraction spikes that would destroy the required contrast and more spiders means more spikes. This sounds bad but, more spiders also means that the spikes move out away from $\rho = 0$. It turns out that with enough spiders the high contrast zone can be preserved. Fig. 3 shows the psf one gets using 100 and 180 spiders.

2.3. Starshape Masks

It seems wasteful to develop a high-throughput concentric-ring mask only to overlay it with a throughput reducing spiderweb obstruction just to offer support. To avoid this waste, we ask whether it is possible simply to adjust the width of the spiders appropriately as a function of radius and dispense with the concentric rings altogether. As shown in Ref. 3, this can be done. We call such masks *starshape* masks. A typical mask of this type is shown in Fig. 4.

The analysis behind starshape masks is very similar to that which leads to Eq. 2. The only changes are that the constant α is now allowed to depend on radius r and that the apodization $A(r)$ is gone:

$$\begin{aligned}
 E(\rho, \phi) \approx & 2\pi \int_0^{1/2} J_0(2\pi r \rho) (1 - N\alpha(r)/(2\pi)) r dr \\
 & - 4 \int_0^{1/2} J_N(2\pi r \rho) \cos(N(\phi - \pi/2)) \sin(N\alpha(r)/2) r dr.
 \end{aligned} \tag{3}$$

Our aim is for the factor $(1 - N\alpha(r)/(2\pi))$, which depends on r , to give the effect of any specified apodization. This is done by setting

$$\alpha(r) = \frac{2\pi}{N} (1 - A(r)).$$

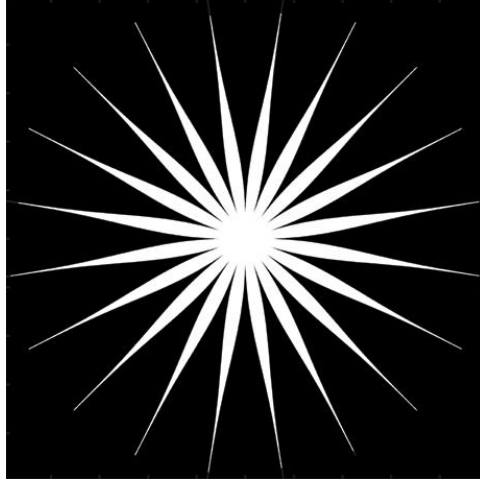


Figure 4. A 20-point (or vane) starshape mask.

The resulting psf turns out to be the psf associated with the apodization overlaid with diffraction spikes caused by using a finite number of vanes. Again, the diffraction spikes move out as N increases and a value of N of about 150 or more gives a sizeable high-contrast discovery zone.

There is a starshape mask associated with every apodization. The question arises as to which apodization we should use. We've already argued that the zero-one valued concentric-ring apodization is in some sense the optimal apodization. But, a zero-one valued apodization implemented as a starshape mask is again just a set of concentric rings and so the issue of how to support the rings resurfaces. One possible solution to this is to put an upper bound on the apodization function that is strictly less than one. In this way, we can prevent there being any rings of openness in the starshape mask. However, such an upper bound reduces throughput which was exactly what motivated us to consider this family of masks. It turns out that one can instead impose smoothness constraints on the apodization function and find a smooth apodization that is arbitrarily close to the zero-one valued apodization in terms of throughput. Smoothness is the approach we follow. Given that the prolate spheroidal wave function looks very much like a Gaussian curve, we impose the following two smoothness constraints that are indeed satisfied by a Gaussian function:

$$(\log A)' \leq 0, \quad (\log A)'' \leq 0.$$

The resulting optimization problem is:

$$\begin{array}{ll} \text{maximize} & \int_0^{1/2} A(r) 2\pi r dr \\ \text{subject to} & -10^{-5} E(0) \leq E(\rho) \leq 10^{-5} E(0), \quad \rho_{iwa} \leq \rho \leq \rho_{owa}, \\ & 0 \leq A(r) \leq 1, \quad 0 \leq r \leq 1/2, \\ & A'(r) \leq 0, \quad 0 \leq r \leq 1/2, \\ & A(r) A''(r) \leq A'(r)^2, \quad 0 \leq r \leq 1/2. \end{array}$$

Fig. 5 shows the optimal apodization computed using $\rho_{iwa} = 4$ and $\rho_{owa} = 60$. The Airy throughput is again 9%. Finally, Fig. 6 shows the psf's for the associated starshape masks with 20 and 150 star points. We see that 20 points is too few and that 150 is adequate to provide a large dark zone in the psf.

2.4. Asymmetric Masks

For comparison with the circularly symmetric masks, we introduce here two asymmetric masks.

Fig. 7 shows the pupil mask based on the prolate spheroidal wave function, which was originally proposed and studied in Ref. 4. It provides high contrast only in a narrow region around the positive and negative x -axis and hence requires a very large number of separate integrations in order to provide coverage of all angles around the central star. On this axis,

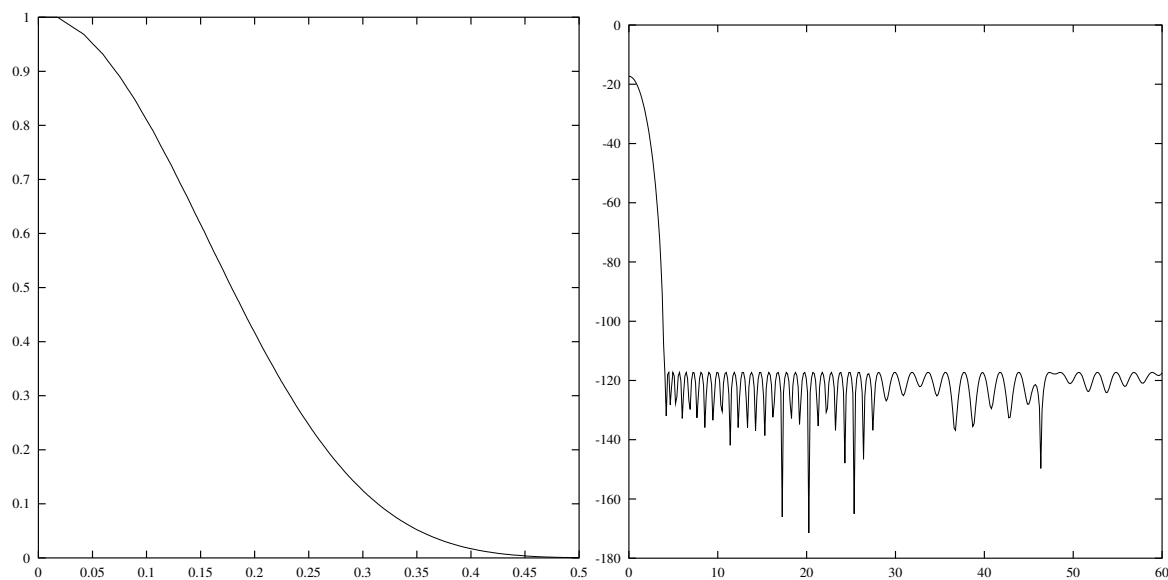


Figure 5. *Left.* The optimal smooth apodization computed using $\rho_{iwa} = 4$ and $\rho_{owa} = 60$. *Right.* The associated psf. Note: the Airy throughput is 9%.

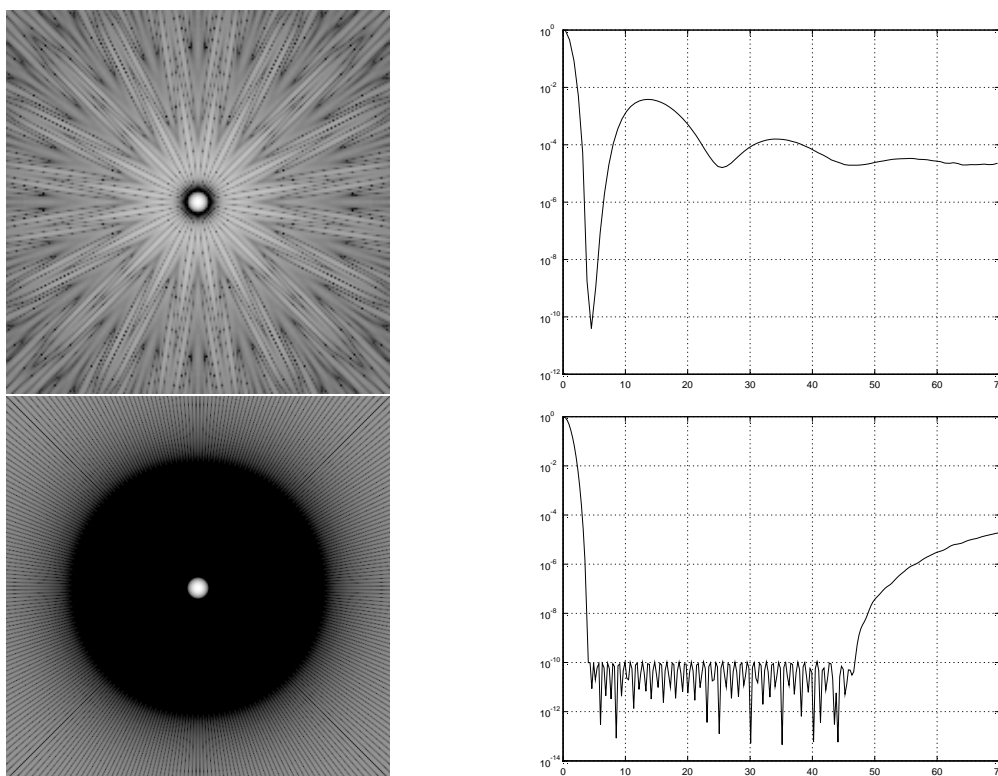


Figure 6. *Top.* The psf for a 20-point starshape mask having $\rho_{iwa} = 4$ and $\rho_{owa} = 60$. *Bottom.* The psf for a 150-point starshape mask having $\rho_{iwa} = 4$ and $\rho_{owa} = 60$. In both cases, the Airy throughput is 9%.

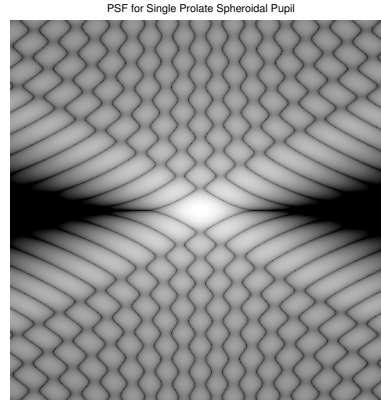
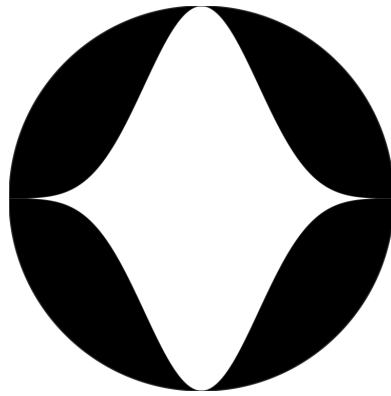


Figure 7. *Left.* A single opening pupil mask designed to provide high contrast in a neighborhood of the x -axis. *Right.* The corresponding psf. On the x -axis, contrast of 10^{-10} extends over $\rho \geq 4$. The Airy throughput is 43%.

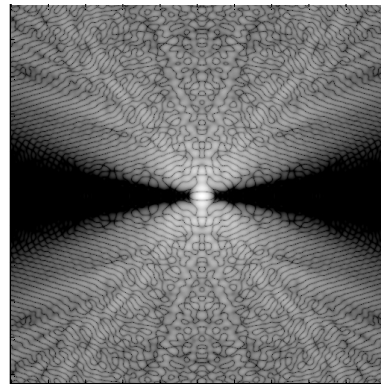
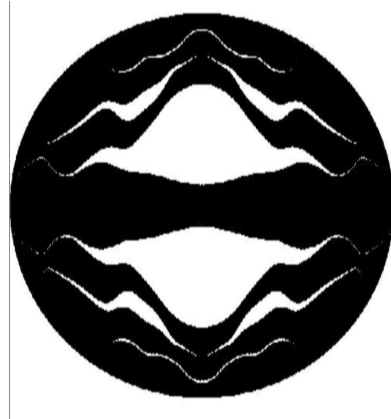


Figure 8. *Left.* A multiopening pupil mask designed to open up the high-contrast region. *Right.* The corresponding psf. On the x -axis, contrast of 10^{-10} extends over $\rho \geq 4$. The Airy throughput is 12%.

the high contrast region extends over $|\rho| \geq 4$. Its small dark zone is partially compensated for by a high Airy throughput of 43%.

Fig. 8 shows a multi-opening pupil mask that was designed to improve somewhat on the narrow high-contrast zone of the previous mask. It can cover all angles around the central star with 10 integrations. Its Airy throughput is 12%.

3. COMPARISONS

Table 1 provides a side-by-side comparison of the masks discussed in this paper. In terms of throughput, the asymmetric masks are the best. But, if the location of a planet is not known, which will be the case during planet-discovery, these masks require a large number of separate integrations in order to cover all angles. Hence, for discovery, the circularly symmetric masks are better whereas for studying a planet in a known location the asymmetric masks are preferred. The starshape mask, if manufacturable, is better than the spiderweb mask but manufacturing compromises might well make these two designs essentially equivalent. For both spiderweb and starshape masks, a small “bead” can be added to the center of the mask to “anchor” the many very fine vanes that converge there. Simulations indicate that the bead can have a radius up to 2% of the radius of the aperture.

	ρ_{iwa}	ρ_{owa}	Airy Thruput	Number of Integrations
Concentric Rings	4	60	9.37	1
Spiderweb with 10% spiders	4	60	7.59	1
Starshape	4	60	9.09	1
Asymmetric Prolate	4	∞	42.66	$\infty?$
Asymmetric Multiple	4	100	11.85	10

Table 1.

Acknowledgements

This work was partially performed for the Jet Propulsion Laboratory, California Institute of Technology, sponsored by the National Aeronautics and Space Administration as part of the TPF architecture studies and also under contract number 1240729. The first author received support from the NSF (CCR-0098040) and the ONR (N00014-98-1-0036).

REFERENCES

1. D. Slepian, "Analytic solution of two apodization problems," *Journal of the Optical Society of America* **55**(9), pp. 1110–1115, 1965.
2. R. Vanderbei, D. Spergel, and N. Kasdin, "Spiderweb Masks for High Contrast Imaging," *Astrophysical Journal* , 2003. To appear.
3. R. Vanderbei, D. Spergel, and N. Kasdin, "Circularly Symmetric Apodization via Starshaped Masks," *Astrophysical Journal* , 2003. Submitted.
4. N. J. Kasdin, D. N. Spergel, and M. G. Littman, "An optimal shaped pupil coronagraph for high contrast imaging, planet finding, and spectroscopy," *submitted to Applied Optics* , 2002.